NeuroImage: Clinical 25 (2020) 102175

Contents lists available at ScienceDirect

NeuroImage: Clinical

journal homepage: www.elsevier.com/locate/ynicl

Aberrant inter-hemispheric coordination characterizes the progression of minimal hepatic encephalopathy in patients with HBV-related cirrhosis

Min Ye[a,b,1], Zheng Guo[c,1], Zhipeng Li[d,1], Xiaoshan Lin[e], Jing Li[d], Guihua Jiang[f], Yun Teng[g], Yingwei Qiu[e,*], Lujun Han[d,**], Xiaofei Lv[d]

[a] Department of Geriatrics, Guangzhou First People's Hospital, School of Medicine, South China University of Technology, Guangzhou, Guangdong, China
[b] Department of Geriatrics, Guangzhou First People's Hospital, Guangzhou Medical University, Guangzhou, Guangdong, China
[c] Department of Oncology, The First Affiliated Hospital of Ganzhou Medical University, Ganzhou, Guangdong, China
[d] Department of Medical Imaging, Sun Yat-sen University Cancer Center, State Key Laboratory of Oncology in South China, Collaborative Innovation Center for Cancer Medicine, Guangzhou, Guangdong, China
[e] Department of Radiology, The Third Affiliated Hospital of Guangzhou Medical University, Guangzhou Medical University, Guangzhou, Guangdong, China
[f] Department of Medical Imaging, Guangdong No. 2 Provincial People's Hospital, Guangzhou, Guangdong, China
[g] Department of Radiology, Lianjiang people' hospital, Zhanjiang, Guangdong, China

ARTICLE INFO

Keywords:
Corpus callosum
Hepatitis-B-virus-related cirrhosis
Minimal hepatic encephalopathy
Resting-state functional MRI
Structural MRI
Voxel-mirrored homotopic connectivity

ABSTRACT

Patients with hepatitis B virus (HBV)-related cirrhosis (HBV-RC) and minimal hepatic encephalopathy (MHE) exhibit alterations in homotopic inter-hemispheric functional connectivity (FC) and corpus callosum (CC) degeneration. However, the progression of inter-hemispheric dysconnectivity in cirrhotic patients from no MHE (NMHE) to MHE and its association with the progression of diseased-related cognitive impairment remain uncharacterized. We hypothesized that inter-hemispheric dysconnectivity exists in NMHE patients and further deteriorates at the MHE stage, which is associated with performance measured by psychometric hepatic encephalopathy scores (PHES) that can characterize cirrhotic patients with NMHE and MHE. Using inter-hemispheric homotopic FC and CC (and its subfields) volumetric measurements in 31 patients with HBV-RC (17 with NMHE and 14 with MHE) and 37 healthy controls, we verified that MHE patients had significant attenuated inter-hemispheric homotopic FC in the bilateral cuneus, post-central gyrus, inferior parietal lobule, and superior temporal gyms, as well as CC degeneration in total CC, CC2, CC3, and CC4 (each comparison had a corrected $P < 0.05$). In contrast, NMHE patients had relatively less severe inter-hemispheric homotopic FC and no CC degeneration. In addition, the degeneration of the CC and inter-hemispheric homotopic functional disconnections correlated with poor PHES performances in all cirrhotic patients (NMHE and MHE). Furthermore, impairment of inter-hemispheric homotopic FC partially mediated the association between CC degeneration and worse PHES performance. Notably, a combination of inter-hemispheric homotopic FC and CC volumes had higher discriminative values according to the area under the curve (AUC) score (AUC = 0.908, $P < 0.001$) to classify patients into MHE or NMHE groups when compared with either alone. Our findings shed light on the progression of inter-hemispheric dysconnectivity in relation to the progression of disease-related cognitive impairment in patients with HBV-RC.

1. Introduction

Neurocognitive impairment is a common complication of hepatitis B virus (HBV)-related cirrhosis (HBV-RC) (Moriwaki et al., 2010). The most serious neuropsychiatric complication of decompensated HBV-RC is hepatic encephalopathy (HE), which is characterized by a wide spectrum of clinical manifestations, ranging from a subtle impairment in mental state to an induced coma (Cordoba, 2011; Moriwaki et al., 2010; Vilstrup et al., 2014). Minimal HE (MHE) is the mildest form of HE. MHE never presents with any obvious signs or symptoms of

* Corresponding author. Y. Qiu, Department of Radiology, The Third Affiliated Hospital of Guangzhou Medical University, Guangzhou Medical University, Guangzhou, 510150, Guangdong, China
** Corresponding author. L. Han, Department of Medical Imaging, Sun Yat-sen University Cancer Center; State Key Laboratory of Oncology in South China; Collaborative Innovation Center for Cancer Medicine, Guangzhou, 510060, Guangdong, China
E-mail addresses: qiuyw1201@gmail.com (Y. Qiu), hanlj@sysucc.org.cn (L. Han).
[1] These three authors contributed to this work equally.

https://doi.org/10.1016/j.nicl.2020.102175
Received 11 September 2019; Received in revised form 26 November 2019; Accepted 10 January 2020
Available online 11 January 2020

clinically overt HE but can be identified with neuropsychological or neurophysiological tests (Cordoba, 2011). However, the diagnostic criterion for MHE has only recently been standardized. MHE has drawn considerable attention in recent years because it is associated with a compromised quality of life (Labenz et al., 2019), deterioration in daily functioning (Ridola et al., 2018), increased risk of falling and traffic accidents (Bajaj et al., 2009; Labenz et al., 2019), as well as a higher risk of progression to overt HE in cirrhotic patients (Wang et al., 2017). Reportedly, 20%–80% of cirrhotic patients with no MHE (NMHE) eventually develop MHE (Ridola et al., 2018; Vilstrup et al., 2014). This suggests that there is a specific relationship between NMHE cirrhotic patients and MHE cirrhotic patients, even though the relationship between these two processes and the progression from NHME to MHE are not well-understood.

In the past several years, MHE-related brain abnormalities have been extensively investigated using functional and structural magnetic resonance imaging (MRI). Altered brain functional connectivity (FC) detected by resting-state functional MRI (rsfMRI) has been considered to be an important mechanism in the development from NMHE to MHE (Zhang and Zhang, 2018). Several studies have revealed that MHE-related progression is not only associated with the functional disconnections among a series of brain areas distributed in bilateral hemispheres (Sun et al., 2018), but is also related to abnormal functional integration of multiple specific sub-networks—such as the dorsal attention network, default-mode network (DMN), salience network, auditory network, and visual network (Chen et al., 2016; Chen et al., 2014; Qi et al., 2012a,b)—and even whole-brain functional networks (Qi et al., 2015; Zhang et al., 2014). For example, by employing rsfMRI and graph-theoretical approaches, Zhang et al. found disrupted whole-brain FC and abnormal small-world properties in cirrhotic patients, and reorganization of brain networks occurred during disease progression from NMHE to MHE (Zhang et al., 2014). Thus, these studies demonstrate that the progression to MHE may arise from disturbed connectivities among a series of brain regions across the entire brain rather than via segregated regional brain abnormalities. Additionally, MRI-based brain structural studies, such as those using diffusion tensor imaging (DTI) and voxel-based morphometry (VBM), have provided robust evidence for macroscopic white matter (WM) atrophy and disrupted microstructural integrity of WM in the corpus callosum (CC) and bilateral hemispheres during the progression of MHE. For instance, using a combination of VBM and DTI, Chen et al. (Chen et al., 2012) showed consistent widespread WM abnormalities—especially in the CC and bilateral WM regions—and portions of these abnormalities were symmetric in patients with HBV-RC without overt HE. Moreover, changes in the CC and multiple brain regions of the bilateral hemispheres were correlated with poor neurocognitive performance. In another study by Chen et al. (Chen et al., 2015), a Bayesian machine-learning method was used to analyze DTI data from cirrhotic patients and revealed increased mean diffusivity (MD) and decreased fractional anistrophy (FA) which were predominantly located in the bilateral frontal lobes, CC, and parietal lobes—that consistently differentiated MHE patients from NMHE patients. Taken together, these findings suggest that cirrhotic brains may suffer from aberrant functional and structural connections between bilateral hemispheres during the progression from NMHE to MHE.

Interhemispheric homotopic FC is regarded as one of the most salient features of the brain's intrinsic functional infrastructure (Stark et al., 2008), which likely reflects the importance of interhemispheric communication to integrate neural circuits underlying coherent cognition and behavior. Voxel-mirrored homotopic connectivity (VMHC) is a novel approach that can be used to investigate interhemispheric FC in a voxel-wise manner (Zuo et al., 2010). VMHC has been widely used to identify aberrant inter-hemispheric FC in various neuropsychological disorders (Qiu et al., 2017; Shan et al., 2018). As the largest WM structure connecting cortical regions of both hemispheres, the CC is crucial for structural interactions between bilateral hemispheres in the human brain (Hoptman and Davidson, 1994). Disrupted CC integrity and/or morphologic changes of the CC may influence interhemispheric structural communications (Qiu et al., 2017). Thus, identifying specific patterns of inter-hemispheric functional and structural dysconnectivity in cirrhotic patients may help to further elucidate the neural mechanisms of MHE-related progression. However, to the best of our knowledge, only one previous study detected interhemispheric interactions in cirrhotic patients via a combination of VMHC and DTI methods (Chen et al., 2014). In this study, Chen et al. found that—compared with data from healthy controls (HCs)—there was aberrant VMHC in multiple brain regions in MHE patients that was associated with WM structural impairment in the CC (Chen et al., 2014). Although aberrant interhemispheric coordination in MHE patients was documented in this study, cirrhotic patients at the NMHE intermediate state were not included. Hence, it remains unclear whether interhemispheric dysconnectivity is linked to the progression from NMHE to MHE.

In the present study, we combined rsfMRI, high-resolution structural MRI, and psychometric hepatic encephalopathy scores (PHES) to investigate interhemispheric homotopic FC, integrity of the CC and its subregions, and neurocognitive function in NMHE patients, MHE patients, and HCs. Based on previous findings of both structural and functional disconnections during the progression of MHE, we hypothesized the following: (1) compared with HCs, patients with NMHE and MHE have impaired interhemispheric coordination (CC morphometric abnormalities and interhemispheric functional disconnection); (2) in cirrhotic patients, impaired interhemispheric coordination contributes to the development of MHE; and (3) these changes in interhemispheric coordination correlate with PHES and may serve as valuable neuroimaging markers for the diagnosis of MHE.

2. Materials and methods

This study was approved by the local Research Ethics Committee, and written informed consent was obtained from each subject prior to the study. A total of 31 cirrhotic patients (26 male; 45.45 ± 10.14 years old; age range, 27–67 years old) were enrolled in this study. Inclusion criteria were as follows: clinically proven cirrhosis via biopsy or on the basis of case history, clinical examination, and biochemical/imaging findings; 18–70 years old; no current or previous symptoms of overt HE; and no MRI contraindications. Patients were excluded if they exhibited any of the following: other neuropsychiatric disorders; uncontrolled endocrine or metabolic diseases; other types of viral hepatitis; positive human immunodeficiency virus status; prior substantial head trauma; left-handedness; bad vision; history of substance or alcohol abuse; or were taking psychotropic medications. All patients underwent a detailed clinical examination. The severity of liver disease was determined according to the Child-Pugh score.

For comparison, 37 HCs (29 male; 45.70 ± 9.249 years old; age range, 30–63 years old)—who were frequency matched to the included cirrhotic patients in terms of age, gender, and education—were recruited through advertising within the community. No HCs had any liver diseases or other systemic diseases. Other exclusion criteria were the same as those applied to cirrhotic patients. Each healthy subject underwent neuropsychological testing prior to the MRI scan on the same day, but no laboratory tests were performed.

3. Neurocognitive tests and MHE diagnosis

The PHES, including five subtests—number connection test A (NCT-A, in seconds), number connection test B (DST, in numbers), digit symbol test (DST, in numbers), serial dotting test (SDT, in seconds), and line tracing test (LTT, measured as the sum of time taken in seconds and the number of errors)—has been recommended by guidelines to evaluate the degree of neurocognitive impairment and to identify MHE in cirrhotic patients (Randolph et al., 2009). As some of the subjects were

not familiar with the English alphabet, the characters in the NCT-B were replaced with Chinese characters in the same order (Lv et al., 2013). The methodology of how to calculate PHES values has been documented in detail elsewhere (Amodio et al., 2008; Lv et al., 2013). In brief, five regression formulas for predicting results from age and education year constructed using data from 133 healthy subjects in a previous study (Lv et al., 2013) were used to predict the expected results of the five neuropsychological tests. For each PHES subset, the difference between the recorded and predicted values was divided by the standard deviation (SD) as follows: a recorded result of ≥ 1 SD above the predicted value was scored as +1; results of 1 SD and 2 SDs below the predicted value were scored as −1 and −2, respectively; and a result equal to or below −3 SDs was scored as −3. The final PHES values were calculated as the sum of the scores from the five tests and ranged between +5 and −15. All participants in the present study completed the PHES test battery after an appropriate demonstration and explanation. According to previous studies (Amodio et al., 2008; Sun et al., 2018), cirrhotic patients with a PHES score ≤ 4 points were considered to have MHE, whereas patients having a PHES score > 4 points were classified as having NMHE.

4. MRI data acquisition

All imaging data were acquired using a 1.5-T MR scanner with a 16-channel neurovascular coil (AchievaNovaDual; Philips Medical Systems, Best, Netherlands). Participants were instructed to remain still with their eyes closed, to not think of anything in particular, and to remain awake during the scanning. Foam padding was used to reduce head motion. Conventional MR imaging sequences, including T1-weighted images [repetition time (TR) = 600 ms, echo time (TE) = 29 ms] and T2-FLAIR images [TR = 6000 ms, TE = 120 ms, and inversion time (TI) = 2000 ms], were used to detect intracranial lesions. Then, an rsfMRI scan with an echo-planar imaging (EPI) sequence and a high-resolution structural MRI scan with a fast field echo (FFE) three-dimensional T1 weighted (3D-T1WI) sequence were sequentially conducted. The imaging parameters were as follows: (1) RsfMRI: TR/TE = 3,000/50 ms, flip angle = 90°, thickness/gap = 4.5/0 mm, acquisition matrix = 64 × 64, field of view (FOV) = 230 × 230 mm^2, 33 axial slices, and 160 time points (8 min); and (2) 3D-T1WI: TR/TE = 25/4.1 ms, flip angle = 30°, acquisition matrix = 231 × 232, FOV = 230 × 230 mm^2, and 160 sagittal slices with no inter-slice gap. For the rsfMRI scan, subjects were instructed to remain still with their eyes closed, to not think of anything in particular, and to remain awake during the scanning. A simple questionnaire was administered immediately after the MRI scan to check for the degree of collaboration.

5. Data Preprocessing

5.1. RsfMRI data preprocessing

RsfMRI data preprocessing was performed using the Data Processing & Analysis of Brain Imaging (DPABI_V3.0_171210, http://rfmri.org/DPABI) based on statistical parametric mapping (SPM8, http://www.fil.ion.ucl.ac.uk/spm), following previous approaches (Chao-Gan and Yu-Feng, 2010; Qiu et al., 2016; Qiu et al., 2017). Refer to the Supplementary Methods for further details.

After quality control, all subjects had minimum absolute translation and rotation (not exceeding 1.5 mm or 1.5°, respectively). Furthermore, the individual mean framewise displacement (FD) was calculated by averaging the relative displacement from every time point for each subject and including it as a covariate in statistical analyses.

5.2. VMHC calculations

We computed the subject-level VMHC using DPABI software according to a previous approach (Zuo et al., 2010). Global differences in VMHC were examined across the whole brain. For each subject, the homotopic FC was computed as the Pearson's correlation coefficient between each voxel's residual time series and that of its symmetrical inter-hemispheric counterpart. Then, correlation values were transformed using Fisher's z scores. The resulting subject-specific VMHC z-score maps were used for subsequent group-level analyses.

5.3. CC volumetric calculations

The volumes of the CC and its sub-regions were calculated using the FreeSurfer software package (http://surfer.nmr.mgh.harvard.edu/,version6.0) according to a previous approach (Qiu et al., 2016; Qiu et al., 2017). The FreeSurfer-based automated procedures for subcortical volumetric measurements of different brain structures have been described elsewhere (Fischl et al., 2002; Qiu et al., 2016). The volume of each brain structure was then calculated by summing all voxels within the structure. Specifically, the CC was automatically identified and segmented into five sections using FreeSurfer, with each section encompassing 20% of the anterior-posterior distance through the CC that broadly corresponded to functional subdivisions, including anterior (CC1), mid-anterior (CC2), middle (CC3), mid-posterior (CC4), and posterior portions (CC5) (Supplementary Fig. 1). The total CC volume was calculated as the sum of the five CC subdivisions. To reduce the influence of individual variations in the CC value, the normalized CC volume (and those of its sub-regions) was derived through dividing the raw volume by the whole brain volume. All images were visually inspected to ensure accuracy of registration, skull stripping, segmentation, and cortical surface reconstruction.

6. Statistical analysis

6.1. Group differences

A one-way ANOVA was employed to detect significant differences in continuous variables, such as demographic data, and motion parameters. Analysis of covariance (ANCOVA) was used to detect differences in whole-brain VMHC and CC volume (as well as its subfields), while controlling for age, gender and education. A Chi-square test was used to determine any differences among the groups in terms of gender. A Kruskal-Wallis test was used to determine differences in PHES among the groups. A Fisher's least-significant difference (LSD) test was used to perform *post-hoc* multiple comparisons (for CC and its subfields, prior to *post-hoc* LSD tests, Bonferroni corrections were applied for multiple comparisons). Two sample t-tests were used to detect significant differences in clinical data between MHE and NMHE groups for normally distributed variables. Mann-Whitney U tests were used to detect significant differences in clinical data between MHE and NMHE groups for non-normally distributed variables. A $P < 0.05$ (two-tailed) was considered to be statistically significant. All statistical analyses were performed using SPSS 23.0 software.

Whole-brain voxel-wise ANCOVA analysis on subject-specific VMHC maps was performed to determine differences in VMHC among the three groups. Subsequently, *post-hoc* t tests were used to examine between-group differences within significant regions detected by ANCOVA, while eliminating the effects of age, gender, education, and head motion by regression. The results were reported at the significant level of a threshold of two-tailed voxel-wise $P < 0.01$ and cluster level $P < 0.05$ with Gaussian Random Field (GRF) correction, with a gray matter mask produced by the group-level symmetrical template average across all subjects.

6.2. Associations between inter-hemispheric connectivity and PHES

Correlation analyses were performed between brain measures and PHES in SPSS to investigate the association between brain inter-hemispheric coherence (VMHC and CC volume) and neuropsychological

performance in all cirrhotic patients (NMHE and MHE). First, for each cirrhotic patient, the mean VMHC values of regions that differed significantly among the three groups (ANCOVA results) were extracted separately using REST (http://resting-fmri.sourceforge.net). Then, spearman correlation analyses were performed between PHES and the four CC volumetric indices and mean VMHC values of each region. A $P < 0.05$ after Bonferroni correction for multiple comparisons (corresponding to 4 CC volumes and 5 VMHC regions) was considered statistically significant. In addition, the associations between inter-hemispheric connectivity and the different components of the PHES [the number connection test A (NCT-A, in seconds) and B (NCT-B, in seconds), the digit symbol test (DST, in numbers), the serial dotting test (SDT, in seconds) and the line tracing test (LTT–time taken in seconds and the number of errors)] were also investigated.

6.3. Mediation analysis of VMHC, CC volume, and PHES

To investigate whether the influence of the reduced volume in CC on neurocognitive impairment was mediated by VMHC in the cirrhotic groups, a mediation analysis (SPSS)—with total CC volume as the independent variable, PHES as dependent variables, and mean VMHC as the mediator—was performed.

6.4. Receiver operator characteristic (ROC) analysis

Multivariate logistic regression and ROC analysis were used to evaluate the ability of brain inter-hemispheric measures showing significant differences in the ANCOVA analysis (total CC volume and mean VMHC values, alone or combined) to distinguish MHE patients from NMHE patients, and the threshold was set at a significance level of $P < 0.05$.

7. Results

7.1. Demographics and clinical characteristics

There were no group differences in age, gender, or formal years of education (Table 1). Group differences in PHES were observed; cirrhotic NMHE patients had significantly worse PHES scores compared with those of HCs, but had better PHES scores compared with those of MHE cirrhotic patients (Table 1). Group differences in mean grey-matter-based VMHC were also observed; cirrhotic MHE patients had significantly lower VMHC compared with those of NMHE patients and HCs, whereas there no differences were detected between the VMHC of NMHE patients and HCs (Table 1).

Disruption of inter-hemispheric homotopic FC in cirrhotic MHE patients and, to a lesser extent, in NMHE cirrhotic patients

Compared with that of HCs, MHE patients had lower inter-hemispheric homotopic FC between the bilateral inferior parietal lobe (IPL), superior temporal gyrus (STG), precentral gyrus (PreCG) extending to the bilateral posterior central gyrus (PoCG), cuneus (CUN) extending to the bilateral lingual gyrus (LING), middle occipital gyrus (MOG), and middle temporal gyrus (MTG; Fig. 1 and Table 2). Compared with that of cirrhotic NMHE patients, MHE patients had a lower inter-hemispheric homotopic FC in similar but less widespread regions, including the bilateral MOG, LING, PreCG, and CUN. Cirrhotic NMHE patients had lower inter-hemispheric homotopic FC between the bilateral MTG and CUN compared with that of HCs (Fig. 1).

7.2. Selective atrophy of the CC in MHE, but not NMHE, cirrhotic patients

The MHE group had a smaller total CC—mainly in the mid-anterior, central, and mid-posterior parts—compared with those of both NMHE patients and HCs. In contrast, cirrhotic NMHE patients did not have any CC subfield atrophy when compared with that of HCs (Fig. 2 and Supplementary Table 1).

7.3. Interhemispheric homotopic FC and CC sub-region volumes correlate with results of neuropsychological tests in all cirrhotic patients (NMHE and MHE)

The mean VMHC values of all of the clusters that showed significant differences by ANCOVA had significant positive correlations with the performance of PHES in all cirrhotic patients ($r = 0.504$, $P = 0.004$; Fig. 3). The normalized total CC volumes had significant positive correlations with the performance of PHES in all cirrhotic patients ($r = 0.517$, $P = 0.003$; Fig. 3). The mean VMHC of each single significant region (bilateral CUN, bilateral PreCG, bilateral IPL, and bilateral STG) revealed by ANCOVA and the CC3 subfield also had significant positive correlations with the performance of PHES in all cirrhotic patients (Fig. 3). We also found inter-hemispheric connectivity correlated with sub-components of the PHES (NCT-A, NCT-B, DST, SDT, and LTT) in all cirrhotic patients (supplementary materials table 3).

7.4. The impact of CC atrophy on PHES performance is partly mediated by inter-hemispheric FC

The total CC volume was associated with PHES performance in all cirrhotic patients. Furthermore, we found inter-hemispheric FC partially (29.2%) mediated the association between total CC and PHES performance in all cirrhotic patients (Fig. 4).

7.5. Classification of MHE in HBV-RC patients using brain inter-hemispheric measures

According to logistic regression models, the ROC curves for mean

Table 1
Demographic, neuropsychological, and neuroimaging characteristics of HCs and cirrhotic patients.

	HCs (n = 37)	NMHE (n = 17)	MHE (n = 14)	P value
Age (year)	45.70 ± 9.249	43.12 ± 8.943	48.29 ± 11.09	0.331
Sex (Male/Female)	29/8	14/3	12/2	0.825
Education level (year)	11.11 ± 2.875	10.71 ± 3.216	9.07 ± 3.731	0.126
Child–Pugh stage (A/B/C)	NA	11/5/1	5/5/4	0.205
Albumin (mg/dl)	NA	37.04 ± 6.159	32.17 ± 6.046	0.036
Total bilirubin (mg/dl)	NA	64.94 ± 9.998	60.24 ± 12.161	0.247
Prothrombin time (s)	NA	15.92 ± 1.963	17.19 ± 3.297	0.194
PHES (−15–5)[a]	0(-3–2)	-1(-3–1)	-5.5(-4–-11)	$<0.001^{*,\dagger,\#}$
Whole-brain VMHC[b]	0.451 ± 0.013	0.414 ± 0.020	0.351 ± 0.022	$0.007^{*,\#}$
Head motion[c]	0.083 ± 0.041	0.096 ± 0.047	0.084 ± 0.069	0.675

Note: MHE, minimal hepatic encephalopathy; NMHE, patients without MHE; HCs, healthy controls; PHES, psychometric hepatic encephalopathy score; ANOVA, analysis of variance. The markers *, †, and # respectively indicate the significant difference in neurological performance between MHE and HC, NMHE and HC, and MHE and NMHE. [a] Indicates median and range. [b] We adjusted for age when performing group comparisons. [c] Head motion was indexed by mean framewise displacement (FD) derived with Jenkinson' s relative root mean square (RMS) algorithm.

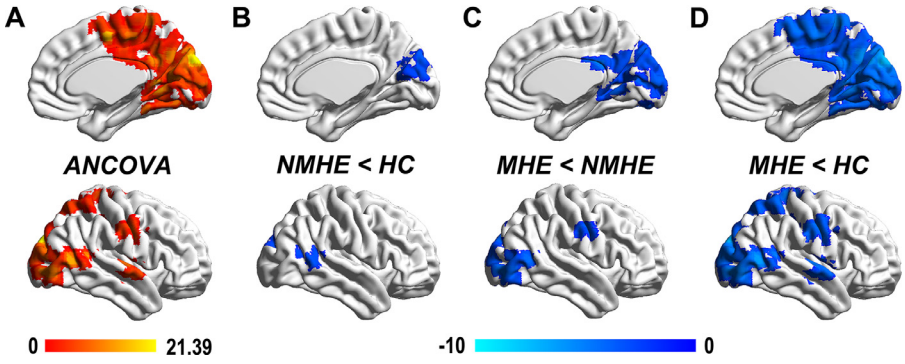

Fig 1. Reduced inter-hemispheric homotopic FC in NMHE and MHE patients. A. After controlling for age, sex, education, and head motion, the three groups showed significant differences in voxel-mirrored homotopic connectivity (VMHC; significant regions highlighted in orange color) in the bilateral inferior parietal lobe (IPL), superior temporal gyrus (STG), precentral gyrus (PreCG) extending to the bilateral posterior central gyrus (PoCG), the bilateral cuneus (CUN) extending to the bilateral lingual gyrus (LING), middle occipital gyrus (MOG), and middle temporal gyrus (MTG) using ANCOVA (color bar represents F-values). **B.** The NMHE group had lower VMHC between the bilateral MTG and CUN compared with that in the healthy control (HC) group (regions highlighted in blue color). **C.** Compared with that of the NMHE group, MHE patients had a lower VMHC in similar but more widespread regions, including the bilateral MOG, LING, PreCG, and CUN. **D.** Compared with that of the HC group, the MHE group had decreased VMHC in more widespread brain regions, which were similar to the regions revealed in ANCOVA results. The blue color bars indicate t-values of each comparison. Statistical significance was set at a height threshold of $P < 0.01$ and cluster threshold of $P < 0.05$ with gaussian random field (GRF) correction. Abbreviations: ANCOVA, analysis of covariance; MHE, minimal hepatic encephalopathy; NMHE, none minimal hepatic encephalopathy; HC, healthy control.

Table 2
Group differences in the inter-hemispheric FC between HCs, NMHE patients, and MHE patients. Statistical significance was set at a height threshold of $P < 0.01$ and cluster threshold of $p < 0.05$ with GRF correction.

Regions	BA	MNI Coordinates			Peak t-score	Cluster size (mm $^{3)}$
		X	Y	Z		
ANCOVA						
CUN/PCUN/CAL/MOG/ LING/MTG/PCC/MFG/STG	6,7,17,18,19,31,39	9	-90	30	21.3875	56862
STG/MTG	21,22	57	-12	3	12.6288	2025
PreCG/PoCG	6	54	-9	36	11.712	4131
SPL/IPL	5,7,40	21	-66	60	9.4745	1701
NMHE < HC						
STG/MTG	21,22	66	-54	9	-3.4437	1674
CUN/PCUN	18,31	15	-78	21	-3.585	4050
MHE < HC						
CUN/PCUN/MOG/MTG/ PCC/MFG	6,7,18,19,31	9	-90	30	-7.2489	55836
STG/MTG	21,22	57	-12	3	-4.9059	1863
PreCG/PoCG	3,4,6	39	-21	39	-4.6387	4077
IPL/SPL/PoCG	5,7,40	21	-66	60	-4.2255	1674
MHE < NMHE						
LING/FG	18,19	18	-27	-21	-4.7336	1350
MOG/MTG/IOG	18,19	39	-90	0	-4.4987	3888
CUN/LING/PCC	17,18,30	12	-54	0	-3.9751	3024
CUN/SOG/PCUN/MOG	7,18,19,31	6	-39	24	-4.6455	5346
PreCG/PoCG	4,6	57	-9	36	-3.8893	1323

Abbreviations: *BA, Broadman area; ANCOVA, analysis of covariance; CAL, calcarine; CUN, cuneus; FG, Fusiform gyrus; HC, healthy control; IPL, inferior parietal lobe; LING, lingual gyrus; MFG, Middle frontal gyrus; MHE, minimal hepatic encephalopathy; MOG, middle occipital gyrus; MTG, middle temporal gyrus; NMHE, none minimal hepatic encephalopathy; PCUN, precuneus; PCC, posterior cingulate cortex; PoCG, posterior central gyrus; PreCG, precentral gyrus; SOG, Superior occipital gyrus; SPL, superior parietal lobule; STG, superior temporal gyrus.*

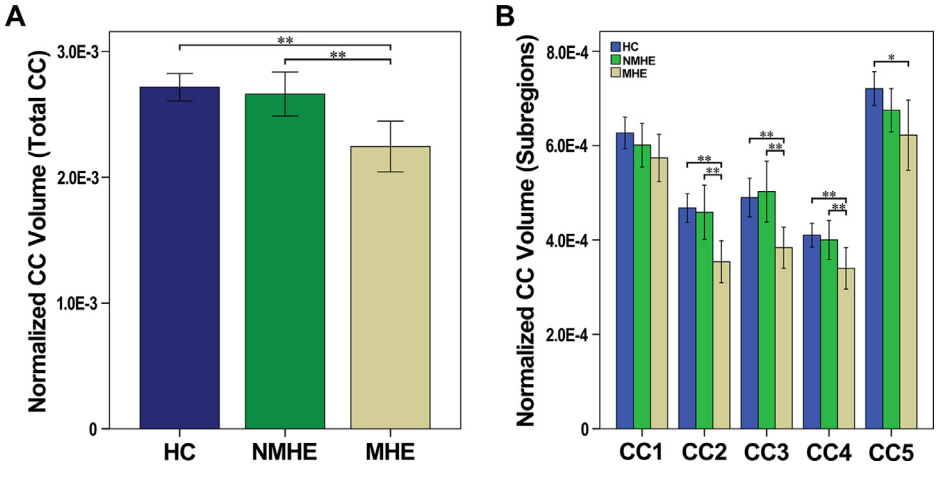

Fig 2. Degeneration of the corpus callosum and its sub-regions in NMHE and MHE patients. (A) After controlling for age, sex, and education, MHE patients had a smaller normalized total CC volume compared with that of NMHE patients and HCs. **(B)** After controlling for age and sex, the MHE group had significantly smaller normalized volumes in the CC2, CC3, and CC4 subregions of the CC compared with those of the HC and NMHE groups. The NMHE group did exhibit any CC subfield atrophy when compared with that of the HC group. Note that '*' indicates the significance level of uncorrected $P < 0.05$, whereas '**' indicates the significance level of $P < 0.05$ (corrected for multiple comparisons). Abbreviations: MHE, minimal hepatic encephalopathy; NMHE, none minimal hepatic encephalopathy; HC, healthy control; CC1, anterior CC; CC2, mid-anterior CC; CC3, Central CC; CC4, mid-posterior CC; CC5, Posterior CC.

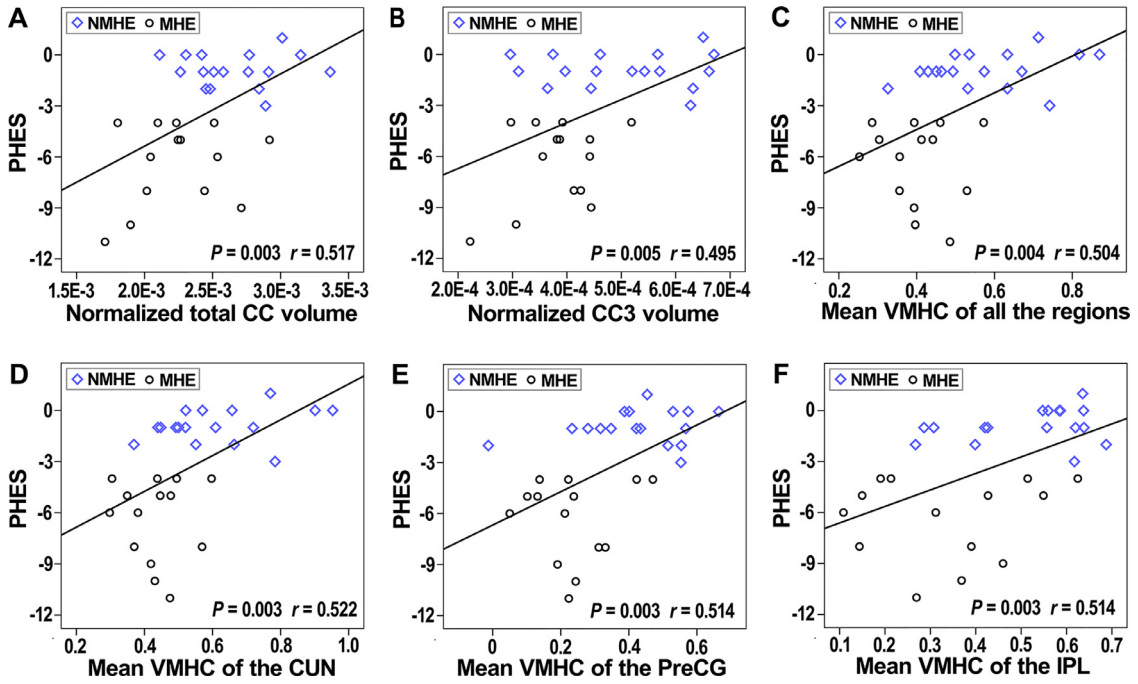

Fig 3. Associations between inter-hemispheric connectivity and PHES. (A, B) The normalized total CC volume and normalized CC3 volume had significant positive correlations with PHES performance in all cirrhotic patients (NMHE and MHE). **(C)** The mean VMHC values of the significantly different regions revealed by ANCOVA had significant positive correlations with PHES performance in all cirrhotic patients (NMHE and MHE). **(D–F)** The mean VMHC of each single region (bilateral CUN, bilateral PreCG, and bilateral SPL) revealed by ANCOVA also had significant positive correlations with the PHES performance in all cirrhotic patients (NMHE and MHE). Abbreviations: CC, corpus callosum; CUN, cuneus; MHE, minimal hepatic encephalopathy; NMHE, none minimal hepatic encephalopathy; PHES, psychometric hepatic encephalopathy score; PreCG, precentral gyrus; SPL, superior parietal lobule; VMHC, voxel-mirrored homotopic connectivity.

VMHC (revealed as having group differences in the ANCOVA) and total CC volume, as well as for combined models, were qualified to determine the efficacies of classification (Fig. 5; Supplementary Table 2). Multivariate regression analysis showed that the logistic regression model combining the two imaging measurements had the highest diagnostic efficiency—based on the area under the curve (AUC) score of the ROC curves (AUC = 0.908, $P < 0.001$)—in distinguishing MHE patients from NMHE patients.

8. Discussion

In the present study, we provided the first-ever examination of inter-hemispheric coordination in both NMHE and MHE HBV-RC patients via a combination of VMHC and CC-segmentation methods. Our findings confirmed that attenuated VMHC was already present in NMHE HBV-RC patients, although no CC degeneration was detected. However, at a later disease stage, MHE HBV-RC patients had more severe inter-hemispheric homotopic functional dysconnectivity and also exhibited CC degeneration (especially in the middle-posterior CC). Interestingly, a reduced VMHC and smaller total CC volume related to PHES performance in all cirrhotic patients. Furthermore, impairment of inter-hemispheric homotopic FC partly (29.2%) mediated the effects of total CC volume on PHES performance in all cirrhotic patients. Moreover, a combination of interhemispheric homotopic FC and CC volume yielded a higher diagnostic value for distinguishing between MHE and NMHE patients when compared with either homotopic FC or CC alone.

The present findings confirmed that MHE is a neurological disease related to disrupted brain connectivity (Chen et al., 2014; Qi et al., 2012a; Zhang et al., 2017; Zhang et al., 2012). Moreover, our findings extend this view to the earlier stages of HBV-RC, in NMHE cirrhotic patients. The present findings provide novel insight into the impact of inter-hemispheric coordination on the PHES performance of both

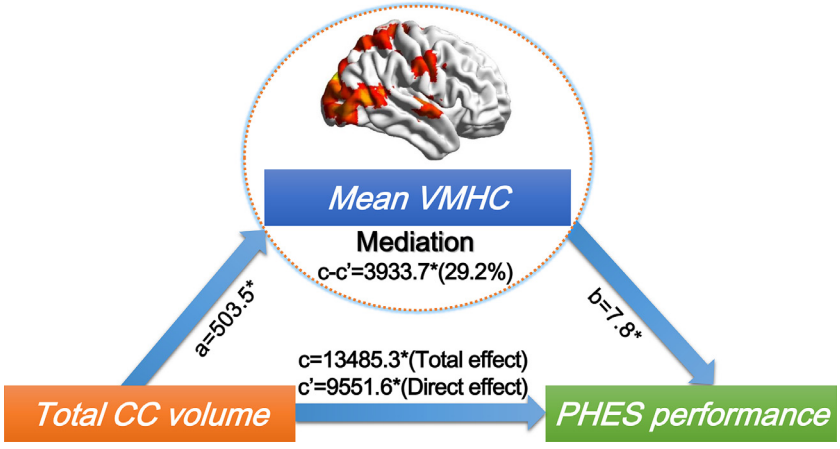

Fig 4. Inter-hemispheric homotopic FC mediates the association of CC degeneration and neurocognitive impairment (PHES performance) in all cirrhotic patients (NMHE and MHE). Regions in which inter-hemispheric homotopic functional connectivity (i.e., VMHC) was related to total CC mediated the impact of total CC degeneration on PHES performance in both NMHE and MHE patients. In the images, "c" denotes the total effect of CC volume on PHES performance; "c'" denotes the direct effect of CC volume on PHES performance (not through inter-hemispheric homotopic functional connectivity); and "c-c'" denotes the indirect effect (mediated effect, through inter-hemispheric homotopic functional connectivity), a denotes coefficient of total CC volume on mean VMHC, while b denotes coefficient of mean VMHC on PHES performances. Note that '*' denotes a significance level of $P < 0.05$. Abbreviations: CC, corpus callosum; MHE, minimal hepatic encephalopathy; NMHE, none minimal hepatic encephalopathy; PHES, psychometric hepatic encephalopathy score; VMHC, voxel-mirrored homotopic connectivity.

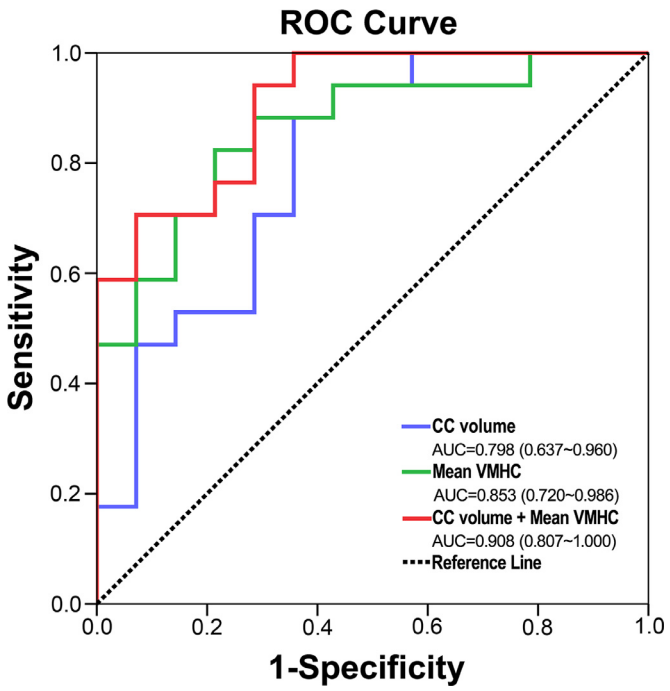

Fig 5. Individual and combined ROC curves for mean VMHC and normalized total CC for determining efficacies in differentiating NMHE and MHE patients. Multivariate regression analysis showed that the logistic regression model combining the two imaging measurements had the highest diagnostic efficiency based on the AUC score of the ROC curves (AUC = 0.908, P < 0.001) in terms of differentiating NMHE and MHE patients. Abbreviations: AUC, area under the curve; CC, corpus callosum; MHE, minimal hepatic encephalopathy; NMHE, none minimal hepatic encephalopathy; ROC, receiver operating characteristic curve; VMHC, voxel-mirrored homotopic connectivity.

NMHE and MHE HBV-RC patients, which may be used to distinguish between MHE and NMHE patients.

Our present study replicates previous results that have shown that inter-hemispheric coordination is compromised in MHE patients. For example, Chen and colleagues found that MHE patients had lower VMHC among bilateral IPL, PoCG, LING, and MOG regions compared with that of normal controls (Chen et al., 2014). Our present study yielded nearly the exact same findings in MHE patients, while the previous study also revealed that the bilateral medial frontal gyrus (MFG), anterior cingulate cortex (ACC), and superior frontal gyrus (SFG) had attenuated FC (Chen et al., 2014). In addition, the same group also found macroscopic atrophy and impairment of microstructural integrity of the CC in MHE patients (Chen et al., 2014; Chen et al., 2012). Another study revealed, via whole-brain VBM analysis, that MHE patients had selective CC atrophy of the middle to posterior regions, although their MHE patients were mixed with alcohol-related cirrhotic patients (Qi et al., 2013). Similarly, we found that MHE patients had attenuated VMHC among bilateral CUN, PoCG, IPL, and STG regions and atrophy of the CC (particularly in middle to posterior regions). Moreover, we extend such findings to the disease's earlier stage, in cirrhotic NMHE patients, although a less severe phenotype was detected (only inter-hemispheric dysfunction, but no volumetric CC abnormalities). Our novel findings suggest that hepatic cirrhosis involves a continuous and progressive increase in inter-hemispheric dysfunction. Since we show that VMHC revealed abnormal inter-hemispheric homotopic FC at the early stage of disease initiation, which deteriorated as the disease progressed, VMHC may represent a sensitive and objective biomarker for tracking disease progression in HBV-RC patients. Of note, we did not detect CC degeneration in NMHE cirrhotic patients. Although inter-hemispheric functional dysconnectivity already existed, it is reasonable to assume that initial inter-hemispheric FC abnormalities would precede structural abnormalities, suggesting that these imaging phenotypes may be indicative of distinct stages of cirrhotic-related brain damage.

Bilateral CUN and MTG homotopic functional connectivity was already compromised in NMHE HBV-RC patients, and such disconnection spread at the MHE stage to the bilateral LING, MOG, MTG, IPL, PreCG, and STG. Visual dysfunction—such as the deficits in visual judgment, visual memory, and visuomotor coordination—is an important and early detectable characteristic of cirrhotic patients without HE (Schiff et al., 2006). As such, it is not surprising that the FC between the bilateral CUN (extending to bilateral LING, MOG, and MTG) and bilateral MTG was compromised in NMHE HBV-RC cirrhotic patients, given that all the above regions are intimately involved in visual information processing (Lee et al., 2000; Wandell et al., 2007) and modulation of top-down visuospatial selective attention (Hahn et al., 2006).

At the MHE stage, the brain regions with compromised FC extended to the PreCG and STG. The PreCG [M1, broadman area (BA) 4 and 6] is intimately involved in motor control and response selection (Duque et al., 2012), while the STG (BA22) is involved in the processing of speech (Ozker et al., 2018). Hence, our results showing a dysfunction in the PreCG and STG are consistent with findings from previous studies that demonstrated the existence of delayed premotor response selection (Schiff et al., 2005) and speech impairment (Bajaj et al., 2011) in MHE patients. Moreover, our differential findings between NMHE and MHE patients indicate that, compared with motor- and speech-related cortices, visual-related cortices may be compromised earlier in hepatic cirrhotic patients. However, the temporal dynamics of region-specific neural deficits require validation in future longitudinal studies.

Interestingly, regional inter-hemispheric homotopic functional dysconnectivity (between the bilateral CUN and MTG) alone may not result in severe PHES abnormalities, which may be due to a reserve capacity elsewhere in the brain (Getz, 2017). Disruption of inter-hemispheric homotopic FC accompanied with CC atrophy would largely disrupt large-scale network interactions and therefore lead to PHES abnormalities in HBV-RC patients (Chen et al., 2016; Zhang et al., 2012). Further analysis in the present study revealed that impairment of interhemispheric homotopic FC partially (29.2%) mediated the effects of CC atrophy on PHES performance in HBV-RC patients. This finding supports general knowledge that neural fibers can influence cognition through neurons, which are the basic structural and functional units of the nervous system. However, our results also suggested that the CC influences cognition through mechanisms that were not quantified by the measurements used here because interhemispheric function only partly mediated such effects (29.2%). Other abnormalities in intra-hemispheric or inter-hemispheric heterotopic FC (inter-hemispheric connections between heterotopic regions) and network architecture might be associated with CC degeneration, which in turn may exert additional impact on PHES performance (O'Reilly et al., 2013; Roland et al., 2017; Shen et al., 2015). Taken together, these findings highlight the importance of structural and functional inter-hemispheric coherence in PHES performance.

In order to overcome the limitations of a single imaging mode, we developed a formula to calculate a combined index for differentiating NMHE and MHE patients. Our combined index was calculated by combining VMHC with CC volumetric data. Our findings indicated that a combination of VMHC and total CC volume yielded the best discriminative value in differentiating NMHE and MHE patients, as compared with VMHC or CC volume alone, suggesting that simultaneous measurements of inter-hemispheric functional and structural connectivities can more comprehensively characterize MHE conditions. The improvement in discrimination power between NMHE and MHE patients may be derived from the fact that inter-hemispheric functional and structural connectivities are complementary and coordinating (Roland et al., 2017; Shen et al., 2015). Notably, the classification power of the combination of inter-hemispheric functional and

structural connectivities should be validated in another independent data in future.

The present study had several limitations. The two primary limitations included the relatively small sample size of the study which limited the statistical power and the relatively low magnetic field strength (1.5 Tesla) of the scanner which had lower signal-to-noise ratio when compared 3.0 Tesla. Future studies with large sample size and higher magnetic field strength (3.0 Tesla or even 7 Tesla) are needed to verify our preliminary results. Second, as a cross-sectional study, we were able to observe abnormal VMHC and CC volumes and their relationship with PHES performance only at one time point in NMHE and MHE cirrhotic patients. As such, our study does not provide any direct evidence for the temporal dynamics or possible causal relationships among CC degeneration, inter-hemispheric functional disconnections, and PHES in disease progression. Future longitudinal studies will be needed to address such temporal dynamics and relationships. Third, as there are no obvious anatomical landmarks to clearly define how to subdivide the CC, we used FreeSurfer to equally subdivide the CC. The main disadvantage of this method was that neither distinct fiber compositions nor fiber connections were accurately reflected in these subregions. Fourth, Although we combined two imaging modes in present study, we only focused on inter-hemispheric functional and structural alterations during the progression of NMHE to MHE, other measurement indices (such as network-related connectivity analysis, and local connectivity metrics, as well as VBM analysis) should be investigated to fully understand the progression of NMHE to MHE in future study. Finally, HBV-related cirrhotic patients, even without MHE, had reduced VMHC, however, whether the aberrant VMHC related to the HBV or cirrhotic is still an open question, further study with detail design is needed to elucidate it.

9. Conclusions

In sum, to our knowledge, this is the first study to demonstrate associations between inter-hemispheric functional and structural coordination, as well as their relationships with PHES performance, in both NMHE and MHE HBV-RC patients. We found that homotopic inter-hemispheric FC disruption already existed in NMHE cirrhotic patients, although no CC atrophy was yet detected. At the MHE stage, patients had more severe homotopic inter-hemispheric FC impairment and initial CC degeneration, suggesting that there are temporal dynamics of inter-hemispheric functional and structural alterations in the disease progression of HBV-RC. Intriguingly, impairment of inter-hemispheric homotopic FC partially mediated the association between CC degeneration and PHES performance in cirrhotic patients. Moreover, a combination of aberrant VMHC and total CC volume yielded higher discriminative value in differentiating NMHE and MHE patients when compared with either alone.

CRediT authorship contribution statement

Min Ye: Writing - original draft, Writing - review & editing. **Zheng Guo:** Investigation, Writing - review & editing. **Zhipeng Li:** Software, Validation. **Xiaoshan Lin:** Visualization, Investigation. **Jing Li:** Data curation, Visualization. **Guihua Jiang:** Investigation. **Yun Teng:** Visualization. **Yingwei Qiu:** Supervision, Conceptualization, Methodology, Writing - review & editing. **Lujun Han:** Software, Writing - review & editing. **Xiaofei Lv:** Data curation, Writing - original draft, Writing - review & editing.

Declaration of Competing Interest

None.

Acknowledgements

This work was funded by grants from the Natural Scientific Foundation of China (grant numbers: 81401399, 81560283, and 81201084), Natural Scientific Foundation of Jiangxi Province, China (grant number: 20151BAB205049), Fundamental Research Funds for the Central Universities of South China University of Technology (Grant number: 2017BQ114), Guangzhou Medical and Health Science and Technology project (20191A010015), and Science and Technology Project of Zhanjiang City (2019B01063). We thank LetPub (www.letpub.com) for its linguistic assistance during the preparation of this manuscript.

Supplementary materials

Supplementary material associated with this article can be found, in the online version, at doi:10.1016/j.nicl.2020.102175.

References

Amodio, P., Campagna, F., Olianas, S., Iannizzi, P., Mapelli, D., Penzo, M., et al., 2008. Detection of minimal hepatic encephalopathy: normalization and optimization of the Psychometric Hepatic Encephalopathy Score. A neuropsychological and quantified EEG study. J. Hepatol. 49 (3), 346–353.

Bajaj, J.S., Cordoba, J., Mullen, K.D., Amodio, P., Shawcross, D.L., Butterworth, R.F., et al., 2011. Review article: the design of clinical trials in hepatic encephalopathy–an International Society for Hepatic Encephalopathy and Nitrogen Metabolism (ISHEN) consensus statement. Aliment Pharmacol Ther 33 (7), 739–747.

Bajaj, J.S., Saeian, K., Schubert, C.M., Hafeezullah, M., Franco, J., Varma, R.R., et al., 2009. . Minimal hepatic encephalopathy is associated with motor vehicle crashes: the reality beyond the driving test. Hepatology 50 (4), 1175–1183.

Chao-Gan, Y., Yu-Feng, Z., 2010. DPARSF: A MATLAB Toolbox for "Pipeline" Data Analysis of Resting-State fMRI. Front Syst Neurosci 413.

Chen, H.J., Chen, Q.F., Liu, J., Shi, H.B., 2016. Aberrant salience network and its functional coupling with default and executive networks in minimal hepatic encephalopathy: a resting-state fMRI study. Sci Rep 627092.

Chen, H.J., Chen, R., Yang, M., Teng, G.J., Herskovits, E.H., 2015. Identification of minimal hepatic encephalopathy in patients with cirrhosis based on white matter imaging and Bayesian data mining. AJNR Am J Neuroradiol 36 (3), 481–487.

Chen, H.J., Wang, Y., Yang, M., Zhu, X.Q., Teng, G.J., 2014. Aberrant interhemispheric functional coordination in patients with HBV-related cirrhosis and minimal hepatic encephalopathy. Metab. Brain Dis. 29 (3), 617–623.

Chen, H.J., Wang, Y., Zhu, X.Q., Cui, Y., Chen, Y.C., Teng, G.J., 2012. White matter abnormalities correlate with neurocognitive performance in patients with HBV-related cirrhosis. J. Neurol. Sci. 321 (1-2), 65–72.

Cordoba, J., 2011. New assessment of hepatic encephalopathy. J. Hepatol. 54 (5), 1030–1040.

Duque, J., Labruna, L., Verset, S., Olivier, E., Ivry, R.B., 2012. Dissociating the role of prefrontal and premotor cortices in controlling inhibitory mechanisms during motor preparation. J. Neurosci. 32 (3), 806–816.

Fischl, B., Salat, D.H., Busa, E., Albert, M., Dieterich, M., Haselgrove, C., et al., 2002. . Whole brain segmentation: automated labeling of neuroanatomical structures in the human brain. Neuron 33 (3), 341–355.

Getz, G.E., 2017. Brain Reserve Capacity (Eds.) In: Kreutzer, J., DeLuca, J., Caplan, B. (Eds.), Encyclopedia of Clinical Neuropsychology. Springer, Cham.

Hahn, B., Ross, T.J., Stein, E.A., 2006. Neuroanatomical dissociation between bottom-up and top-down processes of visuospatial selective attention. Neuroimage 32 (2), 842–853.

Hoptman, M.J., Davidson, R.J., 1994. How and why do the two cerebral hemispheres interact? Psychol. Bull. 116 (2), 195–219.

Labenz, C., Toenges, G., Schattenberg, J.M., Nagel, M., Sprinzl, M.F., Nguyen-Tat, M., et al., 2019. Clinical Predictors for poor quality of life in patients with covert hepatic encephalopathy. J. Clin. Gastroenterol. 53 (7), e303–e307.

Lee, H.W., Hong, S.B., Seo, D.W., Tae, W.S., Hong, S.C., 2000. Mapping of functional organization in human visual cortex: electrical cortical stimulation. Neurology 54 (4), 849–854.

Lv, X.F., Qiu, Y.W., Tian, J.Z., Xie, C.M., Han, L.J., Su, H.H., et al., 2013. Abnormal regional homogeneity of resting-state brain activity in patients with HBV-related cirrhosis without overt hepatic encephalopathy. Liver Int 33 (3), 375–383.

Moriwaki, H., Shiraki, M., Iwasa, J., Terakura, Y., 2010. Hepatic encephalopathy as a complication of liver cirrhosis: an Asian perspective. J Gastroenterol Hepatol 25 (5), 858–863.

O'Reilly, J.X., Croxson, P.L., Jbabdi, S., Sallet, J., Noonan, M.P., Mars, R.B., et al., 2013. Causal effect of disconnection lesions on interhemispheric functional connectivity in rhesus monkeys. Proc Natl Acad Sci U S A 110 (34), 13982–13987.

Ozker, M., Yoshor, D., Beauchamp, M.S., 2018. Converging evidence from electrocorticography and BOLD fMRI for a sharp functional boundary in superior temporal gyrus related to multisensory sspeech processing. Front. Hum. Neurosci. 12141.

Qi, R., Xu, Q., Zhang, L.J., Zhong, J., Zheng, G., Wu, S., et al., 2012a. Structural and functional abnormalities of default mode network in minimal hepatic

encephalopathy: a study combining DTI and fMRI. PLoS One 7 (7), e41376.
Qi, R., Zhang, L.J., Chen, H.J., Zhong, J., Luo, S., Ke, J., et al., 2015. . Role of local and distant functional connectivity density in the development of minimal hepatic encephalopathy. Sci Rep, 513720.
Qi, R., Zhang, L.J., Xu, Q., Zhong, J., Wu, S., Zhang, Z., et al., 2012b. Selective impairments of resting-state networks in minimal hepatic encephalopathy. PLoS One 7 (5), e37400.
Qi, R., Zhang, L.J., Zhong, J., Zhu, T., Zhang, Z., Xu, C., et al., 2013. Grey and white matter abnormalities in minimal hepatic encephalopathy: a study combining voxel-based morphometry and tract-based spatial statistics. Eur. Radiol. 23 (12), 3370–3378.
Qiu, Y., Liu, S., Hilal, S., Loke, Y.M., Ikram, M.K., Xu, X., et al., 2016. Inter-hemispheric functional dysconnectivity mediates the association of corpus callosum degeneration with memory impairment in AD and amnestic MCI. Sci Rep, 632573.
Qiu, Y.W., Jiang, G.H., Ma, X.F., Su, H.H., Lv, X.F., Zhuo, F.Z., 2017. Aberrant inter-hemispheric functional and structural connectivity in heroin-dependent individuals. Addict Biol 22 (4), 1057–1067.
Randolph, C., Hilsabeck, R., Kato, A., Kharbanda, P., Li, Y.Y., Mapelli, D., et al., 2009. Neuropsychological assessment of hepatic encephalopathy: ISHEN practice guidelines. Liver Int 29 (5), 629–635.
Ridola, L., Nardelli, S., Gioia, S., Riggio, O., 2018. Quality of life in patients with minimal hepatic encephalopathy. World J Gastroenterol 24 (48), 5446–5453.
Roland, J.L., Snyder, A.Z., Hacker, C.D., Mitra, A., Shimony, J.S., Limbrick, D.D., et al., 2017. On the role of the corpus callosum in interhemispheric functional connectivity in humans. Proc Natl Acad Sci U S A 114 (50), 13278–13283.
Schiff, S., Mapelli, D., Vallesi, A., Orsato, R., Gatta, A., Umilta, C., et al., 2006. Top-down and bottom-up processes in the extrastriate cortex of cirrhotic patients: an ERP study. Clin. Neurophysiol. 117 (8), 1728–1736.
Schiff, S., Vallesi, A., Mapelli, D., Orsato, R., Pellegrini, A., Umilta, C., et al., 2005. Impairment of response inhibition precedes motor alteration in the early stage of liver cirrhosis: a behavioral and electrophysiological study. Metab. Brain Dis. 20 (4), 381–392.
Shan, Y., Wang, Y.S., Zhang, M., Rong, D.D., Zhao, Z.L., Cao, Y.X., et al., 2018. Homotopic connectivity in early pontine infarction predicts late motor recovery. Front Neurol 9907.
Shen, K., Misic, B., Cipollini, B.N., Bezgin, G., Buschkuehl, M., Hutchison, R.M., et al., 2015. Stable long-range interhemispheric coordination is supported by direct anatomical projections. Proc Natl Acad Sci U S A 112 (20), 6473–6478.
Stark, D.E., Margulies, D.S., Shehzad, Z.E., Reiss, P., Kelly, A.M., Uddin, L.Q., et al., 2008. Regional variation in interhemispheric coordination of intrinsic hemodynamic fluctuations. J. Neurosci. 28 (51), 13754–13764.
Sun, Q., Fan, W., Ye, J., Han, P., 2018. Abnormal regional homogeneity and functional connectivity of baseline brain activity in hepatitis B virus-related cirrhosis with and without minimal hepatic encephalopathy. Front. Hum. Neurosci. 12245.
Vilstrup, H., Amodio, P., Bajaj, J., Cordoba, J., Ferenci, P., Mullen, K.D., et al., 2014. Hepatic encephalopathy in chronic liver disease: 2014 Practice Guideline by the American Association for the Study of Liver Diseases and the European Association for the Study of the Liver. Hepatology 60 (2), 715–735.
Wandell, B.A., Dumoulin, S.O., Brewer, A.A., 2007. Visual field maps in human cortex. Neuron 56 (2), 366–383.
Wang, A.J., Peng, A.P., Li, B.M., Gan, N., Pei, L., Zheng, X.L., et al., 2017. Natural history of covert hepatic encephalopathy: An observational study of 366 cirrhotic patients. World J Gastroenterol 23 (34), 6321–6329.
Zhang, G., Cheng, Y., Liu, B., 2017. Abnormalities of voxel-based whole-brain functional connectivity patterns predict the progression of hepatic encephalopathy. Brain Imaging Behav 11 (3), 784–796.
Zhang, L.J., Zheng, G., Zhang, L., Zhong, J., Li, Q., Zhao, T.Z., et al., 2014. Disrupted small world networks in patients without overt hepatic encephalopathy: a resting state fMRI study. Eur. J. Radiol. 83 (10), 1890–1899.
Zhang, L.J., Zheng, G., Zhang, L., Zhong, J., Wu, S., Qi, R., et al., 2012. Altered brain functional connectivity in patients with cirrhosis and minimal hepatic encephalopathy: a functional MR imaging study. Radiology 265 (2), 528–536.
Zhang, X.D., Zhang, L.J., 2018. Multimodal MR imaging in hepatic encephalopathy: state of the art. Metab. Brain Dis. 33 (3), 661–671.
Zuo, X.N., Kelly, C., Di Martino, A., Mennes, M., Margulies, D.S., Bangaru, S., et al., 2010. Growing together and growing apart: regional and sex differences in the lifespan developmental trajectories of functional homotopy. J. Neurosci. 30 (45), 15034–15043.